CMS Technical Summary Report #90-23

NUMERICAL SIMULATION OF HOLE PRESSURE FOR A JOHNSON-SEGALMAN FLUID

M. Yao and D. S. Malkus

UNIVERSITY OF WISCONSIN

CENTER FOR THE MATHEMATICAL SCIENCES

Center for the Mathematical Sciences
University of Wisconsin—Madison
610 Walnut Street
Madison, Wisconsin 53705

April 1990

(Received April 17, 1990)

Approved for public release
Distribution unlimited

Sponsored by

Air Force Office of Scientific Research
Washington, DC 20332

National Science Foundation
Washington, DC 20550

UNIVERSITY OF WISCONSIN–MADISON
CENTER FOR THE MATHEMATICAL SCIENCES

NUMERICAL SIMULATION OF HOLE PRESSURE FOR A JOHNSON-SEGALMAN FLUID[1]

M. Yao[2] and D. S. Malkus[2]

CMS Technical Summary Report # 90-23
April 1990

ABSTRACT

In this paper we study the hole pressure problem for plane, steady, creeping shear flows of a Johnson-Segalman model. To correctly apply the theory of Higashitani, Pritchard, Baird & Lodge (HPBL), we start with a modified hole pressure relation (MHPR) and we simulate the hole pressure measurement by FEM and multi-mesh extrapolation techniques. The path integrals of MHPR & HPBL are evaluated and a full instrument simulation is conducted.

An encouraging agreement between the simulated hole pressure and the analytical prediction is found, within the computationally-accessible range of $De \lesssim 1$, which supports the postulates about the possible error cancellation in MHPR and the validity of HPBL for J-S fluid. This numerical investigation also corroborates the evidence, given by the independent experiment and other numerical work, that N_1 can be predicted via the HPBL equations to a sufficient approximation to be of practical use.

AMS (MOS) Subject Classifications: 65N99, 73B05, 76-08, 76A05, 76A10.
Key Words: non-Newtonian flows, Couette flow, Poiseuille flow, hole pressure, Johnson-Segalman fluid, HPBL equations, error cancellation, numerical simulation, finite element method, posterior error analysis, multi-mesh extrapolation

[1] Sponsored by the United States Air Force Office of Scientific Research under Grant No. AFOSR-85-0141, the National Science Foundation under grants DMS-8712058 & DMS-8907264 and the UW-Madison Graduate School Research Fund under project number 891533 & 900379.

[2] Also at The Department of Engineering Mechanics.

1. Introduction

The need to measure the first normal stress difference N_1 for viscoelastic liquids has been well recognized in recent years in connection with some important industrial applications. A promising experimental method to measure the elasticity of liquids was proposed and successfully implemented by Lodge *et al.* to estimate N_1 from measured hole pressure P_H for some polymer liquids at various shear rates [1-3]. This method is based on the combination of hole-induced nontrivial curvature of stream surface and base-shear-flow-induced N_1 field. The data analysis of this method depends on the use of the equations of Higashitani, Pritchard, Baird and Lodge (HPBL) whose derivation involves a number of basic assumptions. Extensive discussion of these assumptions can be found in references [1,4,5]

A paradox that had puzzled people in this field for many years, was that at least two of the key assumptions in the HP's original treatment [11] were known to be invalid while the independent experimental tests [1-3,6,7] and published numerical results [4,8-10] have indicated that the HPBL equations are valid to a sufficient approximation to be of practical use. This paradox has been resolved recently by Yao and Malkus [5].

To correctly apply the HPBL theory Yao and Malkus [5] started with a modified hole pressure relation (MHPR) in path integral form. This MHPR contains an extra term which was neglected in Higashitani and Pritchard's original work [11]. By studying the MHPR in streamline co-ordinate formulation Yao & Malkus discovered a fortuitous error cancellation phenomenon in the derivation of HPBL eqations and analytically proved the exact error cancellation for second-order fluid and for Tanner's viscometric model (under some assumptions). It is this error cancellation phenomenon that provides a complete theoretical explanation for the paradox between an apparently flawed derivation and the fortunate success of the HPBL equations.

The proof of the exact error cancellation given by Yao & Malkus in [5] confirms theoretically the validity of HPBL equations for second-order fluid and Tanner's viscometric model. For other non-Newtonian constitutive models, such as the Maxwell and the Johnson-Segalman (J-S) fluids, the analytical proof of the similar error cancellation is still not available. However our numerically-simulated hole pressure results favor this postulate and suggest that the error cancellation phenomenon may be also true for the Maxwell and J-S fluids. Extensive numerical investigations of the hole pressure for the upper-convected Maxwell model have been given by Malkus & Webster in [9] and Yao in [4]. Their investigations corroborate the independent experimental evidence that N_1 can be predicted via HPBL equations to a satisfactory degree of working rheological accuracy.

In this paper we study the hole pressure problem of a modified J-S fluid. The primary goal of this work is to investigate the possible error cancellation phenomenon in the MHPR numerically and to test the validity of the HPBL equations for the J-S model.

The outline of this paper is as follows. In Section 2 we review the basic equations of J-S fluid; in Section 3 we discuss the correct way to derive the HPBL equations, the possible error cancellation in MHPR and the theoretical predictions of hole pressure; in

Section 4 we present our numerical simulation results of P_H and N_1; finally in Section 5 we summarize our conclusions.

2. Basic Equations

Assume the body force is negligible. Then the basic equation governing the motion of an incompressible, isothermal fluid is given by

$$\rho\left(\frac{\partial \mathbf{v}}{\partial t} + \mathbf{v}\cdot\nabla\mathbf{v}\right) = \nabla\cdot\mathbf{T} \tag{2.1}$$

where ρ is the fluid density, $\mathbf{v}$ is the velocity vector, and $\mathbf{T}$ is the Cauchy stress tensor.

In this paper we shall confine our attention to a particular constitutive equation, the J-S model [12] which is actually a nonlinear generalization of the classical Maxwell fluid model. It accounts for the non-affine deformation of Gaussian network by introducing a slip parameter a. Recently there has been growing interest in the modified J-S model with added Newtonian viscosity because it can be used for modeling the non-monotonic stress-strain-rate relation and the ***spurt*** phenomenon [13,14]. In this hole pressure study, however, only the monotonic stress-strain-rate relation is concerned.

The constitutive relation is given by [13]

$$\mathbf{T} = -p\mathbf{I} + 2\eta\mathbf{D} + \Sigma \tag{2.2}$$

where p is an isotropic pressure (which is determined from the incompressibility condition); η is the coefficient of Newtonian viscosity; Σ is the non-Newtonian extra stress; and the strain rate tensor $\mathbf{D} := [\nabla\mathbf{v} + (\nabla\mathbf{v})^T]/2$ is the symmetric part of the velocity gradient $\nabla\mathbf{v}$, which has components $[\nabla\mathbf{v}]_{ij} = \partial v_i/\partial x_j$.

The extra stress is specified by constitutive law of either differential form or integral form. For the differential constitutive law we adopt the same notation as that used in [13,14], i.e.

$$\frac{\Delta\Sigma}{\Delta t} + \lambda\Sigma = 2\mu\mathbf{D} \tag{2.3}$$

where

$$\frac{\Delta\Sigma}{\Delta t} := \frac{\partial\Sigma}{\partial t} + \mathbf{v}\cdot\nabla\Sigma + \Sigma(\mathbf{\Omega} - a\mathbf{D}) + (\mathbf{\Omega} - a\mathbf{D})^T\Sigma \tag{2.4}$$

is the convected time derivative of Σ with parameter a. μ is an elastic shear modulus; λ is a relaxation rate; and the vorticity tensor $\mathbf{\Omega} := [\nabla\mathbf{v} - (\nabla\mathbf{v})^T]/2$ is the antisymmetric part of $\nabla\mathbf{v}$.

In the integral-form of J-S model the extra stress is given explicitly by

$$\Sigma = \frac{\mu_o}{T^2}\int_{-\infty}^{t}\left[\mathbf{E}_t^{-1}(\tau)\mathbf{E}_t^{-T}(\tau) - \mathbf{I}\right]e^{-(t-\tau)/T}d\tau \tag{2.5}$$

where μ_o is the zero shear-rate viscosity, $T = 1/\lambda$ is the relaxation time and we choose $t = 0$ for steady flows. $\mathbf{E}_t(\tau)$ is the effective deformation gradient tensor measuring the strain at

historical time τ relative to the state at t, i.e. $\mathbf{E}_t(\tau) = \partial \mathbf{x}'(\tau)/\partial \mathbf{x}(t)$ with $\mathbf{x}'(\tau)$ and $\mathbf{x}(t)$ being the spatial co-ordinates of the particle positions at time τ and t, respectively.

It can be proved that equations (2.3) and (2.5) are equivalent.

3. Theoretical Predictions of Hole Pressure

Consider steady, incompressible, isothermal, creeping shear flows between parallel walls which are at a separation h. One wall contains a hole whose cross section is a transverse slot (of narrow dimension w parallel to the main flow direction). A transducer centered at point a on the bottom of the hole records an average pressure $P_{a,\mathrm{av}}$, exerted by the fluid. When the hole is deep enough and the inertial effect is negligible, we have $P_{a,\mathrm{av}} = P_a$, where $P_a \equiv -\hat{T}_{22}|_a$ is the point value of normal thrust at a. Another transducer mounted flush with the opposite wall with center on a location b on the hole centerline $\mathbb{C}$ records an average normal thrust $P_{b,\mathrm{av}}$. This arrangement is shown schematically in Figure 1. For slow flows of Newtonian fluids, it is well known that the two readings, P_a and P_b (or $P_{b,\mathrm{av}}$) are the same, i.e. no error is introduced by this procedure. For non-Newtonian fluids, by contrast, the difference between P_a and P_b (or $P_{b,\mathrm{av}}$) can be significant. This difference is called ***hole pressure*** in the literature and is defined in two ways in [1]. One way is to define ***the point (theoretical) value of hole pressure*** by

$$P^{**} = P_b - P_a = -(\hat{T}_{22}|_b - \hat{T}_{22}|_a) \tag{3.1a}$$

where $P_b = -\hat{T}_{22}|_b$ is the point value at b. Another way is to define ***the average (measured) value of hole pressure*** as

$$P^{*} = P_{b,\mathrm{av}} - P_a \ . \tag{3.1b}$$

Definition (3.1a) is convenient for theoretical study while (3.1b) is close to real rheological measurement. In this paper, however, we shall consider the point (theoretical) value of hole pressure only. We shall use P_H, instead of P^{**}, to denote the point value of hole pressure defined by (3.1a). The physical explanation of the existence of hole pressure P_H can be found in references [15,16,1].

3.1 Modified Hole Pressure Relation (MHPR)

As pointed out by Malkus & Yao [17,5], there are two key flaws in the HP's original work [11]. They are

(i) The assumption of $\partial \hat{T}_{11}/\partial q_1 = 0$ on $\mathbb{C}$ is incorrect, due to the excess pressure rise phenomenon observed in [4];

(ii) The assumption of viscometric flow on $\mathbb{C}$ is not true, therefore the change of variable from q_2 to σ_w in getting the rheological space integral (3.10) is invalid in theory.

In order to correctly apply the HPBL theory we need to start with the modified hole pressure relation [17,5] in path integral form:

$$\bar{P}_H = \int_{q_2^a}^{q_2^b} \left(\frac{1}{h_1} \frac{\partial \hat{T}_{11}}{\partial q_1} + \frac{1}{h_2} \frac{\partial \hat{T}_{12}}{\partial q_2} \right) \frac{\hat{T}_{11} - \hat{T}_{22}}{2\hat{T}_{12}} h_2 dq_2 \tag{3.2}$$

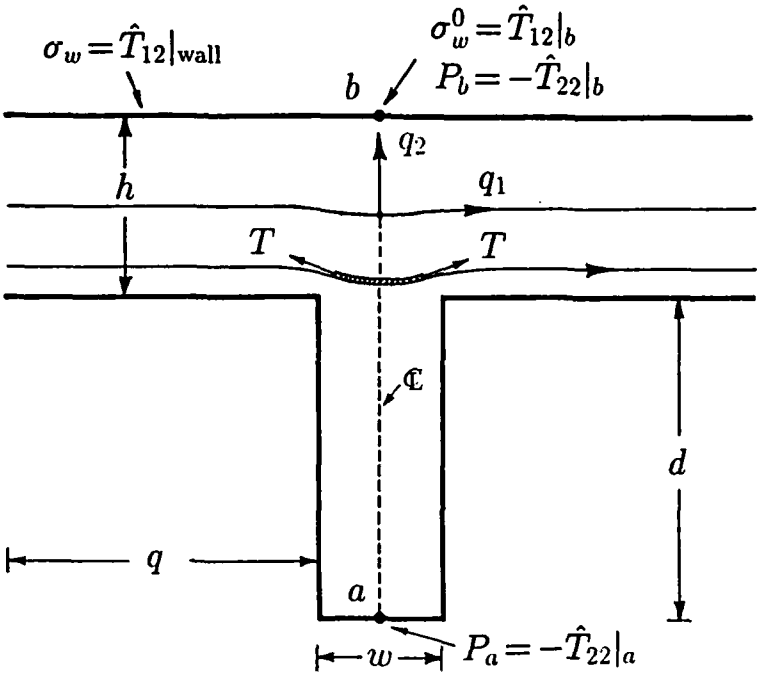

Figure 1. Schematic illustration of hole pressure measurement and definition of streamline coordinate system for planar creeping flows over a transverse slot.

where q_i $(i = 1,2)$ are the strear line co-ordinates defined in Figure 1, h_i $(i = 1,2)$ are the metric factors, and $\hat{T}_{ij}$ $(i,j = 1,2)$ are the physical components of Cauchy stress in streamline co-ordinates. Here we use $\bar{P}_H$ to denote hole pressure predicted by MHPR and to distinguish with the HPBL prediction, P_H. In (3.2) the two key flaws have been corrected by including the stress gradient term $(1/h_1)\partial\hat{T}_{11}/\partial q_1$ and by assuming $\hat{T}_{11} - \hat{T}_{22}$ be generally non-viscometric on $\mathbb{C}$.

Some basic mathematical properties of MHPR, including the singularies and existence of the path integral, have been studied by Yao & Malkus in [5]. Under certain conditions their conclusion theoretically guarantees the existence of the path integral (3.2).

3.2 Error Cancellation and HPBL Equations

Starting from the differential-form constitutive equation (2.3), using the similar orthogonal curvilinear streamline co-ordinate formulation as that was developed in [4,5] and noting the assumed symmetry [5] of velocity field about $\mathbb{C}$, we obtain the physical compo-

nents of the extra stress on the hole centerline $\mathbb{C}$ for the J-S fluid, namely

$$\left.\begin{aligned}\Sigma^{12} &= \frac{\dot\gamma}{1+(1-a^2)T^2\dot\gamma^2}\left[\eta_0+\frac{T^2}{2}\frac{\hat u_1}{h_1}\left((1-a)\frac{\partial\Sigma^{11}}{\partial q_1}\right.\right.\\ &\qquad\left.\left.-(1+a)\frac{\partial\Sigma^{22}}{\partial q_1}\right)-\frac{T}{\dot\gamma}\frac{\hat u_1}{h_1}\frac{\partial\Sigma^{12}}{\partial q_1}\right],\\ \Sigma^{11}-\Sigma^{22} &= 2T\dot\gamma\Sigma^{12}-T\frac{\hat u_1}{h_1}\frac{\partial(\Sigma^{11}-\Sigma^{22})}{\partial q_1},\end{aligned}\right\} \tag{3.3}$$

(3.3) contains streamwise derivatives $\frac{1}{h_1}\frac{\partial\Sigma^{11}}{\partial q_1}$, $\frac{1}{h_1}\frac{\partial\Sigma^{22}}{\partial q_1}$ and $\frac{1}{h_1}\frac{\partial\Sigma^{12}}{\partial q_1}$. In addition, we also need $\frac{1}{h_1}\frac{\partial\hat T_{11}}{\partial q_1}$ in evaluating MHPR. According to our numerical results [4] these derivatives are in general non-zero on the hole centerline $\mathbb{C}$. Equation (3.3) indicates that the flow in general is not strictly viscometric on and in the vicinity of $\mathbb{C}$.

For convenience we rewrite (3.2) as

$$\bar P_H = P_H^1 + P_H^2 \tag{3.4}$$

where

$$P_H^1 = \int_{q_2^a}^{q_2^b}\frac{\hat T_{11}-\hat T_{22}}{2\hat T_{12}}\frac{1}{h_2}\frac{\partial\hat T_{12}}{\partial q_2}h_2\,dq_2\,, \tag{3.5}$$

$$P_H^2 = \int_{q_2^a}^{q_2^b}\frac{\hat T_{11}-\hat T_{22}}{2\hat T_{12}}\frac{1}{h_1}\frac{\partial\hat T_{11}}{\partial q_1}h_2\,dq_2\,. \tag{3.6}$$

The P_H^1 term is similar to the corresponding HPBL equation (but not equal as we shall see) and the P_H^2 is the error term caused by neglecting the stress gradient $(1/h_1)\partial\hat T_{11}/\partial q_1$ in the derivation of HPBL equations.

When expression of $\Sigma^{11}-\Sigma^{22}$ in (3.3) is inserted into (3.5), one obtains

$$P_H^1 = \int_{q_2^a}^{q_2^b}\frac{N_1}{2\hat T_{12}}\frac{\partial\hat T_{12}}{\partial q_2}dq_2 - P_H^3 \tag{3.7}$$

where $N_1 = 2T\dot\gamma\Sigma^{12}$ is the viscometric part of $\Sigma^{11}-\Sigma^{22}$ [4] and

$$P_H^3 = T\int_{q_2^a}^{q_2^b}\frac{\hat u_1}{h_1}\frac{\partial(\Sigma^{11}-\Sigma^{22})}{\partial q_1}\frac{1}{2\hat T_{12}}\frac{\partial\hat T_{12}}{\partial q_2}dq_2\,. \tag{3.8}$$

It is easy to see that if the flow is viscometric on $\mathbb{C}$, then $\partial(\Sigma^{11}-\Sigma^{22})/\partial q_1 = 0$ and hence $P_H^3 = 0$. Therefore P_H^3 can be considered as the error term introduced by the viscometric flow assumption. Our numerical results show that P_H^3 is non-zero in general due to the perturbation of the pressure hole. Furthermore, we shall presume that the HPBL prediction is still valid for the J-S model, i.e.

$$\bar P_H = -\int_{q_2^a}^{q_2^b}\frac{\partial\hat T_{22}}{\partial q_2}dq_2 = \int_{q_2^a}^{q_2^b}\frac{N_1}{2\hat T_{12}}\frac{\partial\hat T_{12}}{\partial q_2}dq_2 = P_H \tag{3.9}$$

where the HPBL prediction of P_H is given by

$$P_H = \int_0^{\sigma_w^0} \frac{N_1}{2\tau} d\tau \ . \tag{3.10}$$

Equation (3.10) is the ***academic form*** of the HPBL equation. Here σ_w^0 is the disturbed wall shear stress at point q_2^b shown in Fig. 1.

Then by using (3.9) and following the way similar to the case of second-order fluid [4,5], one can verify the following relation

$$P_H^2 = P_H^3 \tag{3.11}$$

also holds for the J-S fluid. This suggests the possible error cancellation in the MHPR, namely

$$\bar{P}_H = P_H^1 + P_H^2 = \int_0^{\sigma_w^0} \frac{N_1}{2\tau} d\tau \ \underbrace{- P_H^3 + P_H^2}_{=0} , \tag{3.12}$$

and the equivalence of MHPR and HPBL for J-S fluid. Up to now we have not been able to give a rigorous proof of (3.12) for J-S fluid. To test (3.12) we shall resort alternatively to the numerical simulation technique.

Differentiating bothsides of (3.10) with respect to σ_w^0 and approximating σ_w^0 by σ_w, N_{1w}^0 by N_{1w} yields the ***practical form*** of HPBL equation

$$N_{1w} \doteq 2\sigma_w \frac{dP_H}{d\sigma_w} \tag{3.13}$$

where σ_w is the undisturbed wall shear stress. (3.13) can be considered as a good approximation to the precise differentiation of (3.10) if $|\sigma_w - \sigma_w^0|$ is small. According to Malkus & Webster [9], $|\sigma_w - \sigma_w^0|$ can be minimized by proper die design with $h/w \geq 1$. The full instrument simulation results presented in [4] and in this paper also show that the difference by using either σ_w or σ_w^0 in predicting N_1 is rather small.

The HPBL equations also consider the inertial effect correction [1,2]. Since we are interested only in creeping flows ($Re \approx 0$) the inertial correction term will be neglected in this paper. Thus in the present paper we are actually referring to (3.10) and (3.13) as the HPBL equations.

3.3 An Analytical Prediction of P_H

In reference [18] Yao & Malkus employed an analytical solution technique to predict the hole pressure for J-S fluid. By substituting $N_1 = \frac{2}{1-a^2}\frac{\dot{\gamma}^2}{1+\dot{\gamma}^2}$, $\tau = \epsilon\dot{\gamma} + \frac{\dot{\gamma}}{1+\dot{\gamma}^2}$ into (3.10) and carrying out the integral by changing the variable from τ to $\dot{\gamma}$, they obtained an analytical prediction of P_H, namely

$$\begin{aligned} P_H^* &= \int_0^{\sigma_w^0} \frac{N_1}{2\tau} d\tau = \frac{N_1}{2}\Big|_0^{\sigma_w^0} - \frac{1}{2}\int_0^{\sigma_w^0} \tau d\left(\frac{N_1}{\tau}\right) \\ &= \frac{1}{1-a^2}\left[\frac{\dot{\gamma}^2}{1+\dot{\gamma}^2} - \left(\frac{1}{2}+\epsilon\right)\ln(1+\dot{\gamma}^2) + (1+\epsilon)\ln(1+\epsilon+\epsilon\dot{\gamma}^2)\right]_0^{\dot{\gamma}_w^0} \end{aligned} \tag{3.14}$$

where $\dot{\gamma}_w^0$ is the disturbed shear strain rate $\dot{\gamma}$ on the top wall opposite to the hole, parameter $\epsilon \equiv \lambda\eta/\mu$. Note that in (3.14) $\dot{\gamma}$, τ, N_1, σ_w^0 and $P_H^* = P_H/\mu$ are all in nondimensional form.

There are several important aspects regarding (3.14) that need to be emphasized. It is seen from (3.14) that P_H depends on the value of ratio ϵ. Figure 2(a) & (b) plot the non-dimensional $(1-a^2)P_H/\mu$ vs. $\dot{\gamma}_w^*$ and P_H/N_1 vs. $\dot{\gamma}_w^*$ for $\epsilon = 0,\ 1/8,\ 1/4,\ 1/2,\ 1$, respectively. We can also see that the value of P_H increases with increasing of ϵ, (i.e. when more Newtonian viscosity is added).

We know that both P_H and N_{1w}^0 are equal zero when $\dot{\gamma}_w^0 \to 0$. However the limit of their ratio, P_H/N_{1w}^0, is nontrivial. It can be verified that

$$\lim_{\dot{\gamma}_w^0 \to 0} P_H/N_{1w}^0 = 1/4\ . \tag{3.15}$$

This result is independent of ϵ and can be easily seen from Fig. 2(b). (3.15) shows that the Tanner's second-order fluid result, $P_H = N_{1w}^0/4$, is still a good approximation for very slow flow (small Deborah number) of J-S fluid. By calculating $\lim_{\dot{\gamma}\to\infty} P_H$ it is easy to verify the following asymptotic formula

$$P_H^* \approx \ln\sqrt{1+(\dot{\gamma}_w^0)^2} + \left[1 + (1+\epsilon)\ln\frac{\epsilon}{1+\epsilon}\right] \tag{3.16}$$

for very large De (or $\dot{\gamma}_w^0$).

It is also easy to analytically verify the following differential form HPBL relation holds, namely,

$$N_{1w}^0 = 2\sigma_w^0 \frac{dP_H}{d\sigma_w^0} = 2\sigma_w^0 \frac{dP_H}{d\dot{\gamma}_w^0}\frac{d\dot{\gamma}_w^0}{d\sigma_w^0} \tag{3.17}$$

where $\sigma_w^0 = \epsilon\dot{\gamma}_w^0 + \dot{\gamma}_w^0/[1+(\dot{\gamma}_w^0)^2]$, $N_{1w}^0 = 2(\dot{\gamma}_w^0)^2/(1-a^2)/[1+(\dot{\gamma}_w^0)^2]$ and $P_H = \mu P_H^*$ is given by (3.14).

4. Numerical Simulation

4.1 The FEM Solutions of P_H

The FEM program used in our numerical simulation is FLUCODE, which is implemented with the single-integral form constitutive equation and the particle tracking technique. Early versions of FLUCODE were originally developed by Malkus and his co-workers [19]. The version we used in this work is an enhanced and optimized version developed by the first author [4]. One of the improvement significant for hole pressure simulation is the accuracy improvement of pressure, stress and stress-like variables of FEM solutions at boundary, which is accomplished by the boundary node correction technique [4,20].

The plane Couette base flow as well as the Poiseuille base flow are considered in our numerical simulation. The geometrical parameters, defined in Figure 1, are chosen as

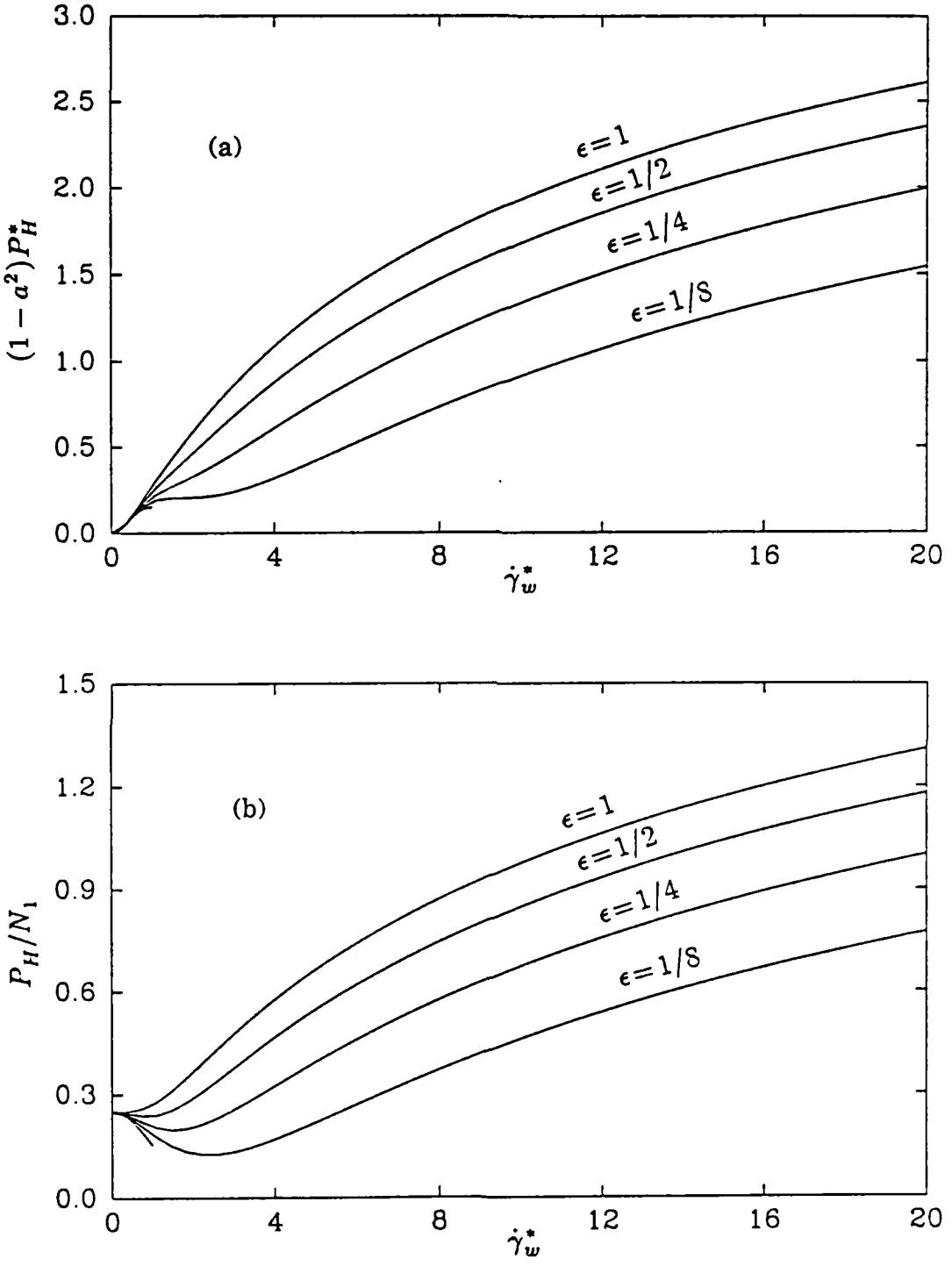

Figure 2.

Analytical prediction of hole pressure error, P_H, of J-S fluid for various values of ϵ. (a) Dimensionless $(1-a^2)P_H^* = (1-a^2)P_H/\mu$ vs. $\dot{\gamma}_w^* = De(1-a^2)^{1/2}$; (b) P_H/N_1 vs. $\dot{\gamma}_w^*$.

$h = 1$, $w = 0.5$, $d = 2$ and $q = 2$. For J-S fluid we hope to get nearly symmetric solutions, but will not impose this. Thus the whole domain is used for the FEM computation.

As for the computational boundary conditions, we specify velocity profiles both at inlet and outlet for the two base flows, plus specifying the upper plate velocity for the Couette base flow. The no-slip boundary conditions are imposed on the remaining portions of the boundary. The fully developed velocity profiles are computed by an analytical solver based on the solution technique and formulation developed in [18]. The FEM computation for mesh 1, 2, 3 was done on a VAX 3100 machine and the computation for mesh 5 was carried out on a Cray X-MP/48 at the San Diego Supercomputer Center.

Five FE meshes are used in the simulation. The first four meshes are designed for multiple-mesh extrapolation [9]. The crudest FE mesh in this group, i.e. Mesh 1, is shown in Figure 3. If Δx_1 is the typical element size of mesh 1, the subsequent meshes have the element sizes $\Delta x_2 = \Delta x_1/2$, $\Delta x_3 = \Delta x_1/3$ and $\Delta x_4 = \Delta x_1/4$, respectively. The last mesh, mesh 5, is specially designed for numerical evaluation of the MHPR and HPBL path integrals. It is the finest one we have ever used on Cray-XMP/48 and is shown in Figure 4.

The material parameters we used are: $a = 0.8$, $\lambda = 1$, $\eta = 1/8$ and $\mu = 1$, which leads to $\epsilon = 1/8$. Five Deborah numbers, i.e. De = 0.1, 0.25, 0.5, 0.75, 1.0, were used. To improve the accuracy of FEM solutions we take $|P_a| = |-\hat{T}_{22}(a)|$, the pressure at the bottom of the hole, as the convergence control variable in determining when to terminate the non-linear iterations for some of the computations at high De. This convergence criterion is proposed by Malkus and is implemented in FLUCODE in the following form

$$|(P_a^i - P_a^{i-1})/P_a^i| < 10^{-n} \tag{4.1}$$

where P_a^i is the i-th iteration solution of P_a and $n = 4$ is used in our computation.

The analytical prediction of the hole pressure P_H, is given by equation (3.14) expressed in terms of the disturbed hole shear strain rate, $\dot{\gamma}_w^0$. The raw FEM solutions of P_H, the HPBL predictions numerically evaluated based on the mesh 5, as well as the extrapolated results of P_H via meshes 1, 2, 3 are compared with the analytical predictions. The numerically-simulated P_H for Poiseuille base flow are summarized in Table 1 and shown in Figure 5 & 6, respectively. It is perhaps necessary to emphasize that although, theoretically, (3.14) is an analytical prediction, in practice we still cannot get the exact values of P_H. This is simply because prediction (3.14) depends on $\dot{\gamma}_w^0$, while the precise value of $\dot{\gamma}_w^0$ is in general unknown for a given base flow. Here the best we can do is to use the most accurate $\dot{\gamma}_w^0$ numerically available for predicting P_H. In Table 1 the $\dot{\gamma}_w^0$ is computed by the three-mesh extrapolation based on meshes 1, 2, 3.

4.2 Evaluation of HPBL and MHPR Path Integrals

A major focus of our numerical work is the investigation of the validity of the HPBL equations and the phenomenon of error cancellation in MHPR for J-S fluid. First it is worth noting that the MHPR path integral (3.2) is based on the streamline co-ordinate

formulation, the stresses involved are the physical stress components in streamline co-ordinates and $\partial/\partial q_1$ is the streamwise derivative. While the FEM solutions obtained from FLUCODE are in the form of Cartesian co-ordinates. An important fact used in our computation is that for the assumed symmetric flow field the streamline co-ordinate systems on $\mathbb{C}$ are orthogonal curvilinear systems and the co-ordinate curves are tangential to the local rectangular Cartesian co-ordinate axes. As defined in reference [21], the physical components of a vector or second-order tensor at a point P relative to a system of orthogonal curvilinear co-ordinates are simply the Cartesian components in a local set of Cartesian axes tangent to the co-ordinate curves through P. Therefore the physical components of $\hat{\mathbf{u}}$ and $\hat{\mathbf{T}}$ are simply the Cartesian components given by the finite element solution.

The differentiation with respect to q_2 is easy, because we can define $q_2 = x_2$, $h_2 = 1$ and there is no direction change for q_2-axis on $\mathbb{C}$. Consequently we have the finite difference formular for $\frac{1}{h_2}\frac{\partial \hat{T}_{12}}{\partial q_2}$ on $\mathbb{C}$

$$\left.\frac{1}{h_2}\frac{\partial \hat{T}_{12}}{\partial q_2}\right|_{q_2^{i+1/2}} = \left.\frac{\partial \sigma_{12}}{\partial x_2}\right|_{x_2^{i+1/2}} \approx \frac{\sigma_{12}(0, x_2^{i+1}) - \sigma_{12}(0, x_2^i)}{x_2^{i+1} - x_2^i} \tag{4.2}$$

where σ_{12} is the Cartesian shear stress component and x_2^i is the x_2-co-ordinate of node i.

However the computation of the streamwise derivatives is much more complicated. As a matter of fact, the computation of $(1/h_1)\partial \hat{T}_{11}/\partial q_1$, etc. is the most difficult part of this investigation; it has turned out to be the most crucial part of the work, too.

To numerically verify the validity of the HPBL equations and the error cancellation phenomenon in MHPR, we compute HPBL, P_H^1, P_H^2 & P_H^3 separately. The numerical procedure used for computing the streamwise derivatives and for evaluating the path integrals are very similar as that described in Section 4.6 of [4]. There are only two major differences between this paper and the Section 4.6 of [4]: namely the symmetry conditions used in there are not valid here and the Cartesian stress components are first transformed into streamline co-ordinate stress components before applying the finite difference formula along the streamline.

The HPBL prediction is evaluated by using the following path integral form:

$$P_H = \int_{q_2^a}^{q_2^b} \frac{N_1}{2\hat{T}_{12}} \frac{\partial \hat{T}_{12}}{\partial q_2} dq_2 \ . \tag{4.3}$$

Here $N_1 = 2T\dot{\gamma}\Sigma^{12}$ is only the viscometric part of $\hat{T}_{11} - \hat{T}_{22}$ given by (3.3) and the trapezoidal rule is used for the numerical integration.

The evaluation of the path integrals of MHPR and HPBL is based on our finest FE mesh, the mesh 5 shown in Figure 4. The numerical results of these path integrals and their relative errors are summarized in Tables 2 & 3 for Couette and Poiseuille base flows, respectively.

In reference [22] Baird, *et al.* have reported a partial self-cancellation phenomenon in evaluating the HPBL path integral (4.3). They found that the contributions to the

HPBL integral from the region below the channel center cancel out. Their observation is primarily based on the experimental data in Poiseuille base flow. Here we find the similar partial self-cancellation in the HPBL path integral based on the numerical solution of J-S fluid.[1] To study the variation of HPBL path integral along $\mathbb{C}$, we define

$$P_H(y) = \int_{q_2^a}^{y} \frac{N_1}{2\hat{T}_{12}} \frac{\partial \hat{T}_{12}}{\partial q_2} dq_2 \qquad q_2^a \le y \le q_2^b \tag{4.4}$$

as a function of parameter y and plot the curve $P_H(y)/P_H(q_2^b)$ vs. y. Note that $P_H = P_H(q_2^b)$ and $y = 0$ is the center of channel. Figure 7(a) shows a $P_H(y)$ curve for Poiseuille base flow at De= 0.25. We can see clearly from Figure 7(a) that $P_H(y) \approx 0$ at $y = 0$, which indicates the self-cancellation of HPBL integral on the interval from the bottom of the hole to the center of the channel. The effective contribution to HPBL integral only comes from the part between the channel center and the top wall where the flow is essentially viscometric. However, this partial self-cancellation phenomenon only happens to Poiseuille base flow; it is not true for the Couette base flow. A typical $P_H(y)$ curve for Couette base flow at De=0.25 is shown in Figure 7(b) which looks quite different from Figure 7(a). It seems that for Couette base flow the most effective contribution to HPBL comes from the part around the mouth of pressure hole.

4.3 Predictions of N_1 – Full Instrument Simulation

The direct application of hole pressure study is the prediction of N_1. In reference [9] Malkus & Webster performed a full instrument simulation to predict N_1 for a Maxwell fluid. Here we conduct a similar simulation for J-S fluid.

In the real rheometric measurement, as done by Lodge & de Vargas in [3], the slit die version of the well-known Weissenberg equation [23]

$$\dot{\gamma}_w = \frac{2Q}{wh^2}\left(2 + \frac{d\ln Q}{d\ln \sigma_w}\right) \tag{4.5}$$

was used to evaluate the shear strain rate $\dot{\gamma}_w$ at the die wall from the volume flow rate Q. Here w denotes the width of the die cross-section and σ_w is the wall shear stress. When simulated by plane flow we can simply take Q/w as the plane flow rate. By using the central difference formula in (4.5) we obtain its finite difference version

$$\dot{\gamma}_w|_{1/2} \doteq \frac{1}{h^2}\left[2(Q_1 + Q_2) + \frac{Q_2 - Q_1}{\sigma_2 - \sigma_1}(\sigma_1 + \sigma_2)\right] . \tag{4.6}$$

With $\dot{\gamma}_w|_{1/2}$, the viscosity function $\eta(\dot{\gamma})$ can be predicted via

$$\eta(\dot{\gamma}_w|_{1/2}) \doteq (\sigma_1 + \sigma_2)/(2\dot{\gamma}_w|_{1/2}) . \tag{4.7}$$

[1] Note that this partial self-cancellation phenomenon also happens to the second-order and Maxwell fluids.

The numerically predicted viscosity is shown in Figure 8.

Following Malkus [9], we take shear stress at the wall to be the independent parameter. Central differences are employed to compute the derivatives and other quantities at shear stress $\bar{\sigma}$, namely

$$\begin{aligned} \bar{\sigma} &= (\sigma_1 + \sigma_2)/2 \ , \\ P_H(\bar{\sigma}) &\doteq [P_H(\sigma_1) + P_H(\sigma_2)]/2 \ , \\ dP_H(\bar{\sigma})/d\sigma &\doteq [P_H(\sigma_2) - P_H(\sigma_1)]/\Delta\sigma \ , \\ Q(\bar{\sigma}) &\doteq [Q(\sigma_1) + Q(\sigma_2)]/2 \ . \end{aligned} \tag{4.8}$$

Using the above approximations, equation (3.13) becomes

$$N_1(\bar{\sigma}) \doteq 2\bar{\sigma}[P_H(\sigma_2) - P_H(\sigma_1)]/\Delta\sigma \ . \tag{4.9}$$

The results of full instrument simulation using (4.9) are presented in Figure 9 and in Table 4, respectively.

5. Conclusions

The numerical results presented in Section 4 show an encouraging agreement between the numerically-simulated hole pressure and the analytical prediction (3.14) for the modified J-S model within the Deborah number range that is computationally accessible. This favors the postulates we made in this paper, namely *the error cancellation in MHPR seems to hold and the HPBL equations are still valid for the J-S fluid.*

The error cancellation relation, $\bar{P}_H = P_H^1 + P_H^3$, has been numerically verified for both Couette and Poiseuille base flows with reasonable degree of accuracy. The numerical results presented here support our conclusion made in [17,4,5] that the flow on $\mathbb{C}$ is not strictly viscometric and in general $P_H^3 \neq 0$, which indicates that the viscometric flow assumption does contribute some error to the path integral P_H^1 and hence $P_H^1 \neq P_H$. This is especially true for the Poiseuille base flow.

However our numerical results also indicate that the error introduced by the viscometric flow assumption, namely the term P_H^3, is not significant for the Couette base flow. As a matter of fact, this error is very small for the second-order fluid (about 2% at $De \doteq 0.2$ [4]); is relatively small for the Maxwell [4] and for J-S fluids at low Deborah numbers (e.g. about 6% at $De = 0.25$ for J-S fluid); and is growing with increase of De (e.g. the error of P_H^1 is about 13% at $De = 1.0$ for a J-S fluid). *The point is that although the effect of non-viscometric flow on $\mathbb{C}$, i.e. the term $\frac{1}{h_1}\frac{\partial(\Sigma^{11}-\Sigma^{22})}{\partial q_1}$, is in general non-zero on $\mathbb{C}$, its contribution to the path integral, P_H^3 defined by (3.8), may be negligible for Couette base flow in some cases. This suggests that the viscometric flow assumption made by Higashitani & Pritchard in* [11] *is indeed a good approximation for Couette base flow of second-order fluid, it perhaps can also be considered as a reasonable approximation for Maxwell & J-S fluids at low Deborah numbers. However our numerical results show that the viscometric flow assumption is not valid for the Poiseuille base flow.* These results support to some extent the Higashitani and Pritchard's original work in [11],

which they clearly intended to apply to Couette base flow. Unfortunately, by neglecting the error terms without estimating them first, they were unable to observe the fortuitous error cancellation phenomenon in the MHPR.

The numerical evaluation of P_H^2 turned out to be the most difficult part of the work because it involves the streamwise stress gradient term, $\frac{1}{h_1}\frac{\partial \hat{T}_{11}}{\partial q_1}$. By using an elaborate numerical procedure we have made some success in evaluating P_H^2. Our numerical results of P_H^2 do have the same sign and the same order of magnitude as those of P_H^3, which does indicate the possibility of the expected error cancellation. However we are still not able to numerically verify the error cancellation relation, $\bar{P}_H = P_H^1 + P_H^2$, to a satisfactory degree of accuracy. Since the values of P_H^3 are checked by relation $\bar{P}_H = P_H^1 + P_H^3$, we suspect the accuracy of P_H^2 is probably still not good enough. The problem is due to the FLUCODE's piecewise-constant FEM stress field which is actually not differentiable in the classic sense. The possible resolution for this problem is to use higher-order FE element with continuous pressure & stress field, or to turn to some other semi-analytical-type methods. This part of work will be pursued in future.

A partial self-cancellation phenomenon in the HPBL path integral on the interval from the bottom of the hole to the center of channel has been observed numerically for the Poiseuille base flow of the J-S fluid. This indicates that the effective contribution to HPBL integral (4.3) only comes from the part between the channel center and top wall where the flow is essentially viscometric. Our observation agrees with what reported by Baird *et al* in [22]. However this partial self-cancellation phenomenon does not happen to Couette base flow.

As we observed from the numerical results, the values of directly computed hole pressure difference $-(\hat{T}_{22}^b - \hat{T}_{22}^a)$ based on mesh 5 are still not good enough. We believe this is due to the slow, possibly fractional-order convergence rate of the thrust $\hat{T}_{22}^a$ at the bottom of the hole discussed in [4]. One the other hand, ***the posterior error analysis base on the multi-mesh extrapolation tells us that the values of*** $-(\hat{T}_{22}^b - \hat{T}_{22}^a)$ ***will indeed be very close to the analytical prediction (3.14) when*** $\Delta x \to 0$. However in order to numerically obtain the desired values of $-(\hat{T}_{22}^b - \hat{T}_{22}^a)$ the FE mesh must be extremely fine, which is propably not achievable in practice, because of the slow convergence rate for $-\hat{T}_{22}^a$. We believe that previous attempts to compare direct computations of $-(\hat{T}_{22}^b - \hat{T}_{22}^a)$ to the HPBL predictions (Bernstein & Malkus [24], Bernstein, Malkus & Olsen [25], Malkus quoted in [16]) were inaccurate due to the very slow convergence of $\hat{T}_{22}^a$ with mesh refinement and not a failure of HPBL. We have suggested severial ways of improving the numerical predictions of FLUCODE:

a) Using pressure smoothing scheme with boundary node correction as standard practice.

b) Using multi-mesh extrapolation.

Or

c) Using the HPBL path integral in place of direct thrust calculations.

From Table 4 we can see that ***the error of predicted*** N_1 ***by means of numerically***

simulated hole pressure measurement is less than 10% when $De \leq 1$. This supports the conclusion made by Malkus & Webster in [9] that N_1 can be predicted via P_H to working rheological accuracy.

According to our computational experience, by setting the P_a-norm convergence criterion (4.1), the accuracy of hole pressure of FEM solutions can be improved to some extent. This criterion is recommended for the hole pressure calculations using FLUCODE.

6. Acknowledgement

The authors acknowledge the support from the Air Force Office of Scientific Research under Grant AFOSR-85-0141, the National Science Foundation under Grants DMS-8712058 & DMS-8907264, the UW-Madison Graduate School Research Fund under project numbers 891533 & 900379 and the San Diego Supercomputer Center.

REFERENCES

[1] Lodge, A.S., in **Rheological Measurement**, edited by A.A. Collyer and D.W. Clegg, Elsevier, London, (1988) Chapter 11.

[2] Lodge, A.S., An attempt to measure the first normal-stress difference N_1 in shear flow for a polyisobutylene/Decalin solution "D2b" at shear rates up to $10^6\ s^{-1}$, *J. Rheology*, 33 (6) (1989) 821-841.

[3] Lodge, A.S. and de Vargas, L., Positive hole-pressures and negative exit pressure generated by molten low-density polyethylene flowing through a slit die, *Rheologica Acta* 22 (1983) 151-170.

[4] Yao, M., A numerical and analytical study of normal stresses and pressure differences in non-Newtonian creeping flows, *Ph.D. Thesis*, University of Wisconsin-Madison, Wisconsin, U.S.A. (1989).

[5] Yao, M. and Malkus, D.S., Cancellation of errors in the Higashitani-Pritchard treatment of hole pressures generated by viscoelastic liquids in creeping flow past a transverse slot, RRC Report #122, Rheol. Research Ctr., Univ. Wisconsin-Madison, also submitted to *Rheol. Acta* (1990).

[6] Pike, R. D. and Baird, D. G., Evaluation of the Higashitani and Pritchard analysis of the hole pressure using flow birefringence, *J. Non-Newtonian Fluid Mech.* 16 (1984) 211.

[7] Baird, D.G., Read, M.D. and Reddy, J.N., Comparison of flow birefringence data with a numerical simulation of the hole pressure, *J. Rheology*, 32(6) (1988) 621-638.

[8] Webster, M.F., The hole-pressure problem, *Rheologica Acta*, 23 (1984) 582-590.

[9] Malkus, D.S. and Webster, M.F., On the accuracy of finite element and finite difference predictions of non-Newtonian slot pressures for a Maxwell fluid, *J. Non-Newtonian Fluid Mech.*, 25 (1987) 93-127.

[10] Sugeng, F., Phan-Thien, N. and Tanner, R.I., A boundary-element investigation of the pressure-hole effect, *J. Rheology*, 32 (3) (1988) 215-233.

[11] Higashitani, K. and Pritchard, W.G., A kinematic calculation of intrinsic errors in pressure measurements made with holes, *Trans. Soc. Rheology* 16 (1972) 687-696.

[12] Johnson, M.W. Jr. and Segalman, D., A model for viscoelastic fluid behavior which allows non-affine deformation, *J. Non-Newtonaian Fluid Mech.*, **2** (1977) 255-270.

[13] Malkus, D.S., Nohel, J.A. and Plohr, B.J., Dynamics of shear flow of a non-Newtonian fluid, *J. Comput. Phys.* (to appear), also Tech. Summary Report # 89-14, Ctr. Math. Sci., Univ. of Wisconsin-Madison (1988).

[14] Malkus, D.S., Nohel, J.A. and Plohr, B.J., Quadratic dynamical systems describing phenomena in shear flow of non-Newtonian fluids, *Proceedings IMA Workshop on Nonlinear Evolution Equations that Change Type*, Springer-Verlag, also Tech. Summary Report # 90-7, Ctr. Math. Sci., Univ. of Wisconsin-Madison (1989).

[15] Pipkin, A.C. and Tanner, R.I., A survey of theory and experiment in viscometric flows of viscoelastic liquids, **Mechanics Today**, Vol. 1, edited by S. Nemat-Nasser, Pergamon, (1972) 262-321.

[16] Bird, R.B., Armstrong, R.C. and Hassager, O., **Dynamics of Polymeric Liquids**, Vol. 1 **Fluid Mechanics**, *2nd edn.*, John Wiley & Sons (1987).

[17] Malkus, D.S. and Yao, M., On hole-pressure in plane Poiseuille flow over transverse slots, Tech. Summary Report # 2943, Math. Research Ctr., Univ. Wisconsin-Madison (1986).

[18] Yao, M. and Malkus, D.S., Analytical solution of plane Poiseuille flow of a Johnson-Segalman fluid, submitted to *J. Non-Newtonian Fluid Mech.* (1990).

[19] Malkus, D.S., Finite element methods for viscoelastic flow, in **Viscoelasticity and Rheology**, edited by A.S. Lodge, M. Renardy, J.A. Nohel, Academic Press (1985) 391-419.

[20] Yao, M. and Malkus, D.S., Boundary node correction and superconvergence in the FEM, *Int. J. Numer. Methods Fluids*, to appear (1990).

[21] Malvern, L.E., **Introduction to the Mechanics of a Continuous Medium**, Prentice-Hall, (1969).

[22] Baird, D.G., Malkus, D.S. and Reddy, J.N., Comparison of flow birefringence results with numerical simulation of the hole pressure, *Proceedings IX Intl. Congress on Rheol.*, Mexico (1984) 641-646.

[23] Walters, K., **Rheometry**, Chapman & Hall, London: Wiley, New York (1975) eqn. (5.54) p. 105.

[24] Bernstein, B., Malkus, D.S. and Olsen, E.T., A finite element for incompressible plane flows of fluids with memory, *Int. J. Numer. Methods Fluids*, **5** (1985) 43-70.

[25] Malkus, D.S. and Bernstein, B., Flow of a Curtiss-Bird fluid over a transverse slot using the finite element drift-function method, *J. Non-Newtonian Fluid Mech.*, **16** (1984) 77–116.

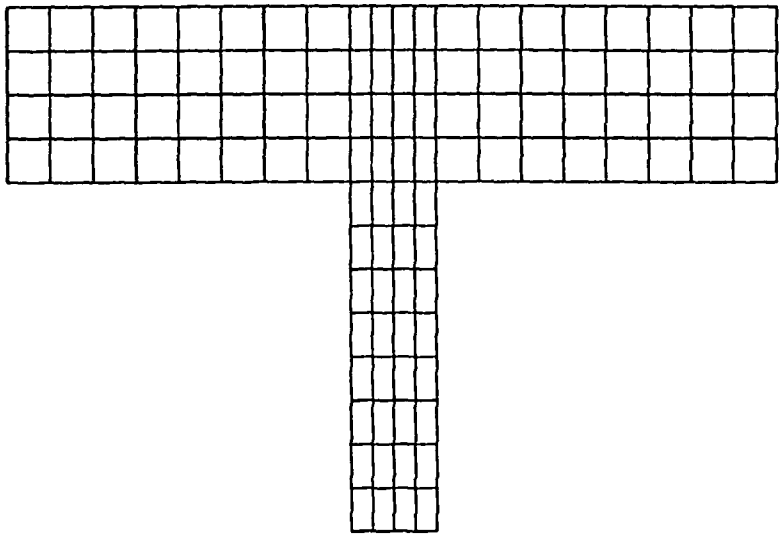

Figure 3. Crudest FEM mesh, i.e. the Mesh 1 of the four-mesh group for multiple mesh extrapolation. The other three finer FEM grids are obtained by even subdivision of this mesh in each co-ordinate direction.

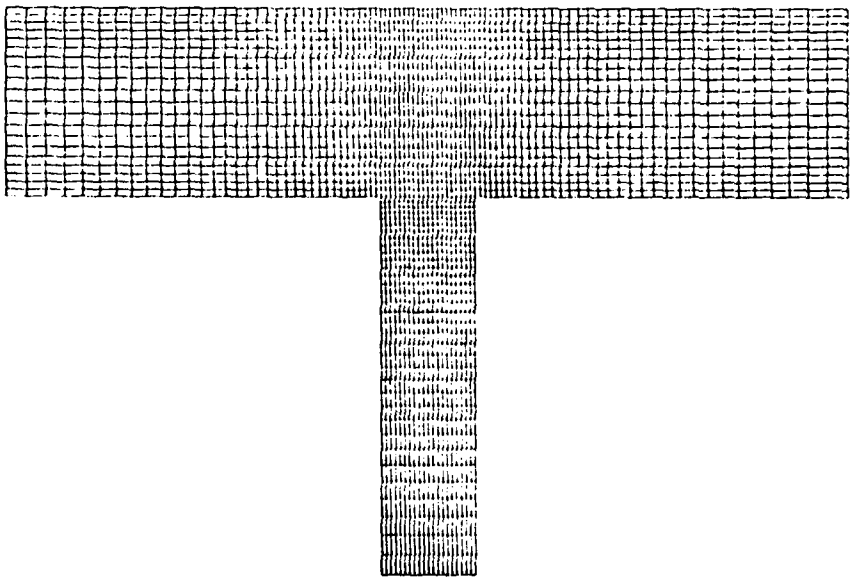

Figure 4. The Mesh 5 used for numerical evaluation of MHPR. This is the finest mesh we used with 2440 quadrilateral macro elements and 2583 nodes.

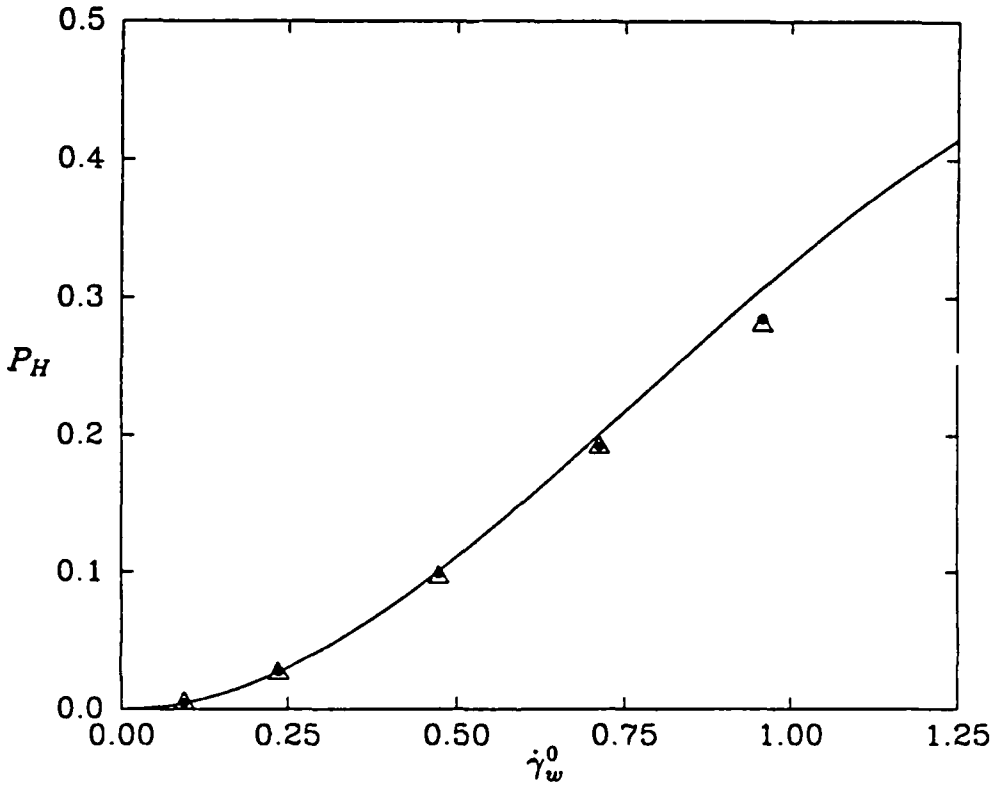

Figure 5.

Hole pressure error for plane Poiseuille base flow of a modified J-S fluid ($\epsilon = 1/8$). Numerical simulation vs. analytical prediction. The solid curve is the analytical predction calculated by (3.14); Δ is the extrapolated values of P_H based on meshes 1, 2 and 3; $\bullet$ is computed by the HPBL path integral (4.3) based on mesh 5.

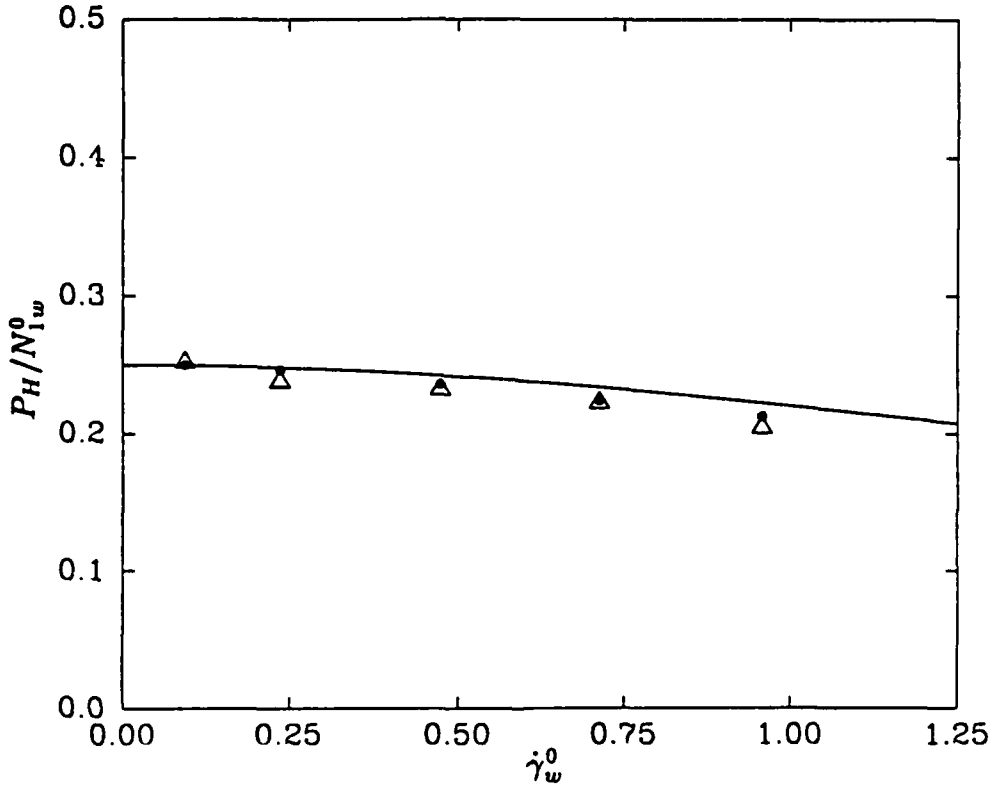

Figure 6.

P_H/N_{1w}^0 for plane Poiseuille base flow of a modified J-S fluid ($\epsilon = 1/8$). Numerical simulation vs. analytical prediction. The solid curve is the analytical predction calculated by (3.14); Δ is the three-mesh extrapolation result using meshes 1, 2 and 3; $\bullet$ is the HPBL path integral result (4.3) based on mesh 5.

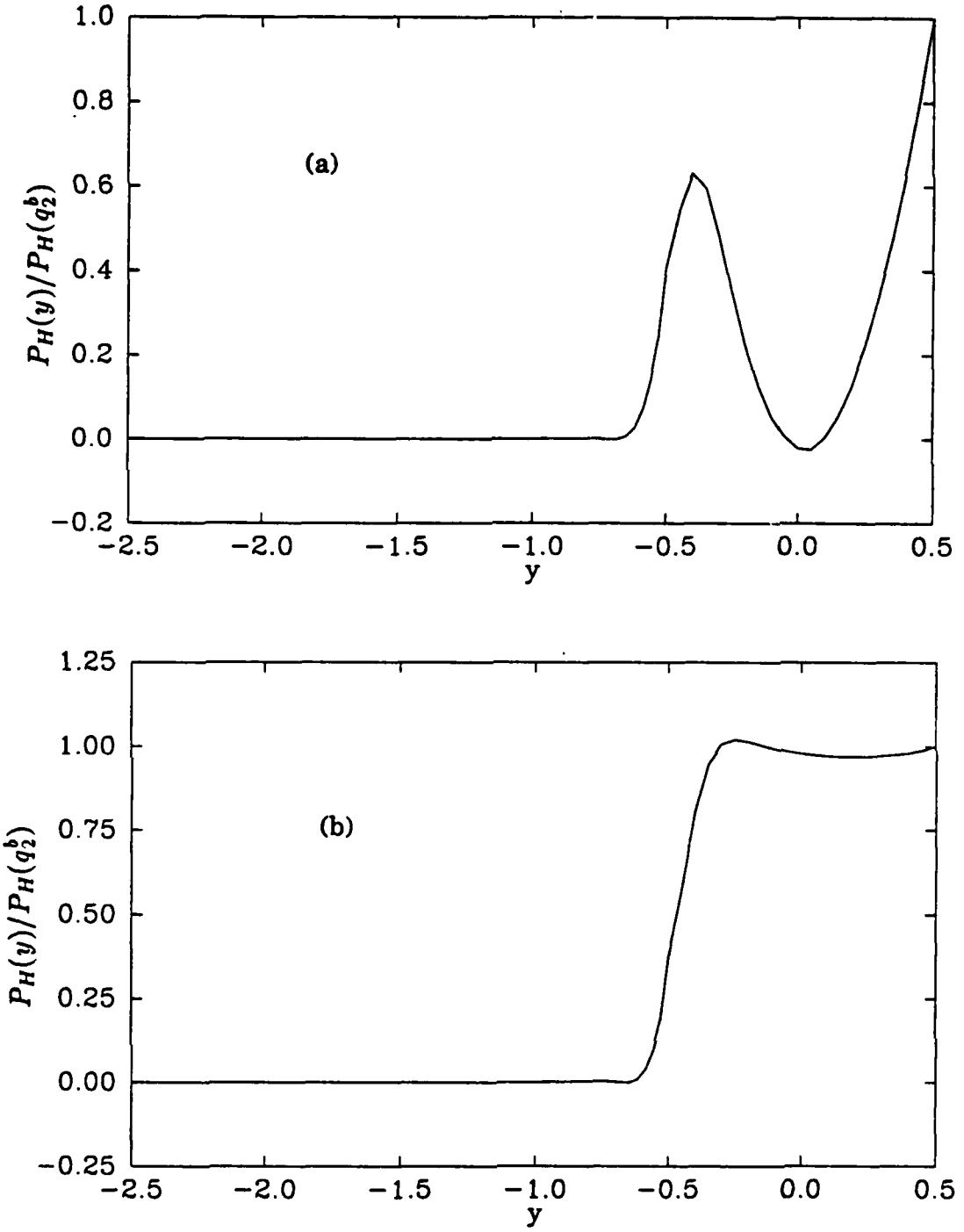

Figure 7.

Variations of the HPBL path integral, $P_H(y)$, along the hole centerline $\mathbb{C}$. (a) $P_H(y)/P_H(q_2^b)$ vs. y for Poiseuille base flow at De $= 0.25$; (b) $P_H(y)/P_H(q_2^b)$ for Couette base flow at De $= 0.25$. Note that $y = -2.5$ is the bottom of pressure-hole and $y = 0$ is the center of channel.

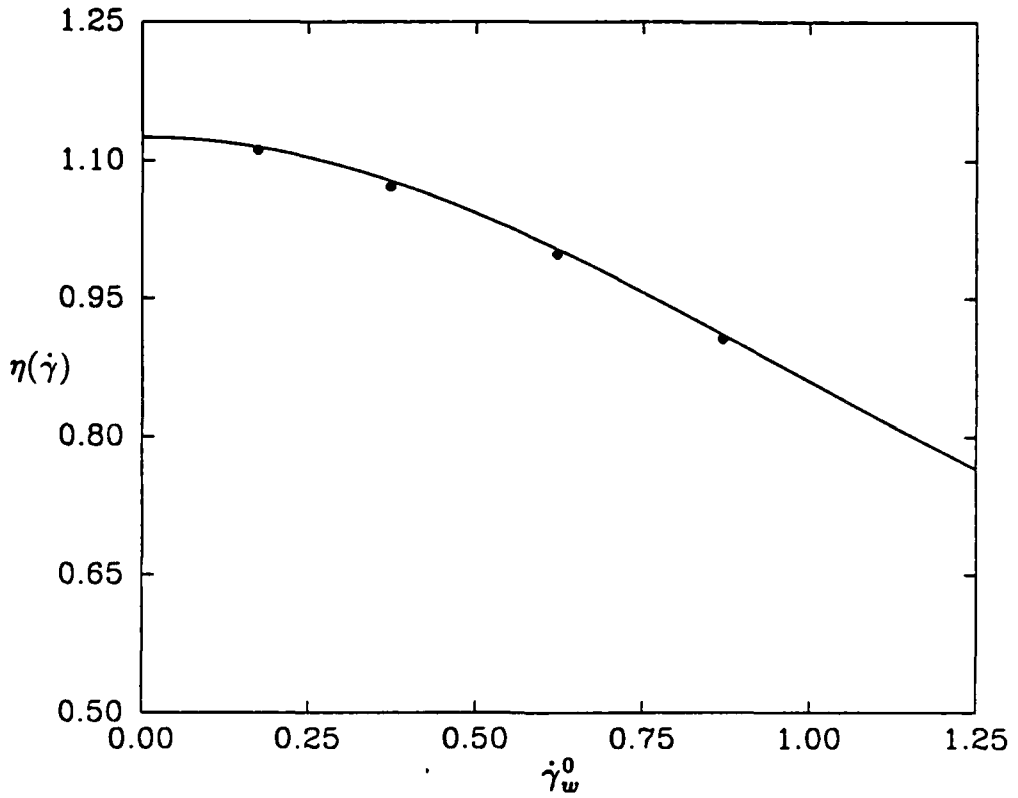

Figure 8.

Numerical predictions of viscosity at $\epsilon = 1/8$, using the three-mesh extrapolations of FEM solutions. The solid curve is the analytical function of viscosity $\eta(\dot{\gamma}) = \epsilon + 1/[1 + (1 - a^2)T^2\dot{\gamma}^2]$; and • is the value predicted by equations (4.6) & (4.7).

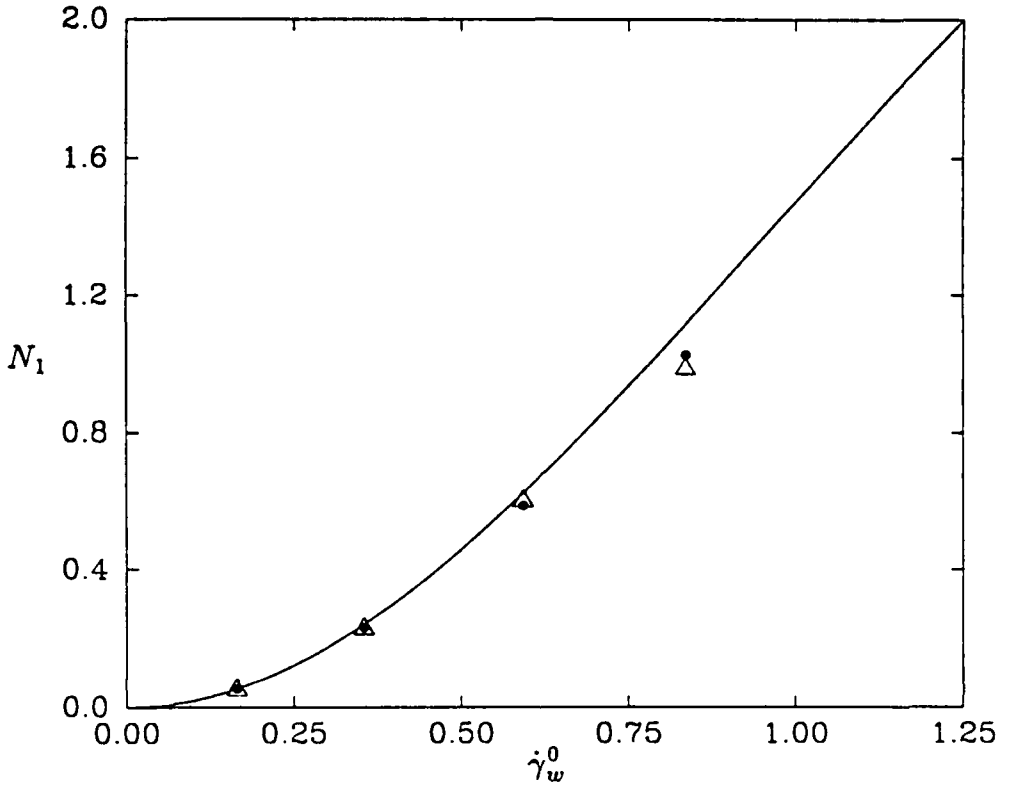

Figure 9.

Predictions of N_1 based on the simulated hole pressure measurement, using the J-S model and (4.9). The solid curve is the analytical solution; • is the predicted value using P_H = HPBL path integral; Δ is predicted by using extrapolated P_H based on meshes 1, 2, 3.

(a) P_H Extrapolated by Meshes 1, 2, 3

De	$\dot{\gamma}_w^{0*}$	P_H^*	P_H	Error
0.10	.094783	.0044718	.0045146	0.96%
0.25	.23661	.027226	.026023	−4.42%
0.50	.47350	.10060	.096237	−4.34%
0.75	.71227	.20053	.19126	−4.62%
1.00	.95788	.30684	.28034	−8.64%

(b) Raw P_H from Mesh 5

De	$\dot{\gamma}_w^{0*}$	P_H^*	P_H	Error
0.10	.094783	.0044718	.0034648	−22.52%
0.25	.23661	.027226	.022362	−17.87%
0.50	.47350	.10060	.085607	−14.90%
0.75	.71227	.20053	.16776	−16.34%
1.00	.95788	.30684	.24855	−19.00%

(c) HPBL Prediction Based on Mesh 5

De	$\dot{\gamma}_w^{0*}$	P_H^*	HPBL	Error
0.10	.094783	.0044718	.0045526	1.81%
0.25	.23661	.027226	.027484	0.95%
0.50	.47350	.10060	.098875	−1.71%
0.75	.71227	.20053	.19179	−4.36%
1.00	.95788	.30684	.28474	−7.20%

Table 1.

Numerically-simulated hole pressure for plane Poiseuille base flow of a Johnson-Segalman fluid ($\epsilon = 1/8$) by FEM solutions. $\dot{\gamma}_w^{0*}$ denotes the perturbed shear strain rate at q_2^b and its value is obtained through three-mesh extrapolation based on meshes 1, 2, 3. P_H^* is the analytical prediction computed via equation (3.14) with $\dot{\gamma}_w^0 = \dot{\gamma}_w^{0*}$. HPBL is the path integral prediction (4.3) based on FEM solutions of mesh 5.

Table 2.

Numerical Evaluation of MHPR (3.2) in Path Integral Form and Error Cancellation for Couette Base Flow of J-S Fluid ($\epsilon = 1/8$, De $= 0.25,\ 0.5,\ 1.0$)

Deborah Number	De = 0.25	De = 0.5	De = 1.0
F.E. Mesh	Mesh 5	Mesh 5	Mesh 5
F.E. Number	NE= 2440	NE= 2440	NE= 2440
F.E. Size	$\Delta x = 0.025$	$\Delta x = 0.025$	$\Delta x = 0.025$
$-(\hat{T}_{22}\|_b - \hat{T}_{22}\|_a)$	.020291	.081376	.27466
Analytical P_H	.032302	.11723	.33530
P_H^1	.034449	.12817	.37792
$(P_H^1 - P_H)/P_H$	6.65%	9.33%	12.71%
P_H^3	−.0042013	−.018105	−.073182
$P_H^1 + P_H^3$	.030248	.11006	.30473
error of $P_H^1 + P_H^3$	−6.36%	−6.12%	−9.11%
$P_H = \int_{q_2^a}^{q_2^b} \frac{N_1}{2\hat{T}_{12}} \frac{\partial \hat{T}_{12}}{\partial q_2} dq_2$	.031980	.11328	.31762
error of P_H	−1.00%	−3.37%	−5.27%

Table 3.

Numerical Evaluation of MHPR (3.2) in Path Integral Form and Error Cancellation for Poiseuille Base Flow of J-S Fluid ($\epsilon = 1/8$, De $= 0.25,\ 0.5,\ 1.0$)

Deborah Number	De = 0.25	De = 0.5	De = 1.0
F.E. Mesh	Mesh 5	Mesh 5	Mesh 5
F.E. Number	NE= 2440	NE= 2440	NE= 2440
F.E. Size	$\Delta x = 0.025$	$\Delta x = 0.025$	$\Delta x = 0.025$
$-(\hat{T}_{22}\|_b - \hat{T}_{22}\|_a)$	.022362	.085857	.24855
Analytical P_H	.027226	.10060	.30684
P_H^1	.053771	.20474	.64770
$(P_H^1 - P_H)/P_H$	97.50%	103.52%	111.09%
P_H^3	−.030839	−.11727	−.40571
$P_H^1 + P_H^3$	.022932	.087470	.24198
error of $P_H^1 + P_H^3$	−15.77%	−13.05%	−21.14%
$P_H = \int_{q_2^a}^{q_2^b} \frac{N_1}{2\hat{T}_{12}} \frac{\partial \hat{T}_{12}}{\partial q_2} dq_2$	.027484	.098875	.28474
error of P_H	+0.95%	−1.71%	−7.20%

	Using σ_w and $P_H = \int_{q_2^a}^{q_2^b} \frac{N_1}{2\hat{T}_{12}} \frac{\partial \hat{T}_{12}}{\partial q_2} dq_2$			
De	$\dot{\gamma}_w^0$	$N_1(\dot{\gamma}_w^0)$	$N_1^{\text{predicted}}$	Error
0.175	0.16570	0.05437	0.05434	−0.06%
0.375	0.35506	0.24118	0.23177	−3.90%
0.625	0.59289	0.62405	0.58769	−5.83%
0.875	0.83508	1.11484	1.02677	−7.90%
	Using σ_w^0 and $P_H = \int_{q_2^a}^{q_2^b} \frac{N_1}{2\hat{T}_{12}} \frac{\partial \hat{T}_{12}}{\partial q_2} dq_2$			
De	$\dot{\gamma}_w^0$	$N_1(\dot{\gamma}_w^0)$	$N_1^{\text{predicted}}$	Error
0.175	0.16570	0.05437	0.05435	−0.04%
0.375	0.35506	0.24118	0.23052	−4.42%
0.625	0.59289	0.62405	0.57168	−8.39%
0.875	0.83508	1.11484	0.98559	−11.59%

Table 4.

Comparison of predicted N_1 with the analytical solution $N_1(\dot{\gamma}_w^0)$ for Poiseuille base flow of J-S fluid. Here $\dot{\gamma}_w^0$ and σ_w^0 are the disturbed wall shear-strain-rate and total shear stress on $\mathbb{C}$; σ_w is the undisturbed total wall shear stress; $P_H = \int_{q_2^a}^{q_2^b} \frac{N_1}{2\hat{T}_{12}} \frac{\partial \hat{T}_{12}}{\partial q_2} dq_2$ is the HPBL prediction in path integral form; $N_1^{\text{predicted}}$ is computed via (4.9) by using σ_w & P_H and σ_w^0 & P_H, respectively.